THE MICROSCOPE • Vol 57:4, pp 157-163 (2009)

Aerodynamic Stability and the Growth of Triangular Snow Crystals

K.G. Libbrecht and H.M. Arnold
Department of Physics, California Institute of Technology*

KEYWORDS

Snow crystals, crystal growth, crystal morphology, ventilation effect, diffusion-limited growth, growth instabilities, crystal faceting, Monte Carlo simulation

ABSTRACT

We describe laboratory-grown snow crystals that exhibit a triangular, plate-like morphology, and we show that the occurrence of these crystals is much more frequent than one would expect from random growth perturbations of the more-typical hexagonal forms. We then describe an aerodynamic model that explains the formation of these crystals. A single growth perturbation on one facet of a hexagonal plate leads to air flow around the crystal that promotes the growth of alternating facets. Aerodynamic effects thus produce a weak growth instability that can cause hexagonal plates to develop into triangular plates. This mechanism solves a very old puzzle, as observers have been documenting the unexplained appearance of triangular snow crystals in nature for nearly two centuries.

INTRODUCTION

Complex patterns and structures often emerge spontaneously when crystals grow, yielding a great variety of faceted, branched and other forms. This is readily seen, for example, in the well-known morphological diversity found in naturally occurring mineral crystals (1). Suppressing structure formation is often desired when growing large commercial crystals, but exploiting the phenomenon provides a route for using nanoscale self-assembly as a possible manufacturing tool (2). Whether the goal is to reduce, enhance or otherwise control, there has been considerable interest from a number of fronts in characterizing and understanding the detailed physical mechanisms that produce ordered structures from disordered precursors during solidification (3, 4).

The molecular dynamics involved in the condensation of disordered molecules into a regular crystalline lattice is remarkably complex, involving a number of many-body effects over different length scales and time scales (5). As a result, calculating dynamical properties, such as crystal growth rates, from first principles is generally not yet possible. Predicting growth morphologies has also proven quite difficult, with few overarching theories connecting the many disparate physical mechanisms that govern growth behaviors.

A well-known and often-studied example of structure formation during crystal growth is the formation of ice crystals from water vapor. In the atmosphere, these are called snow crystals, and they fall from the clouds with a remarkable variety of morphologies, including simple plate-like and columnar forms, elaborately branched plates, hollow columns, capped columns and many others (6). We have been studying the detailed physics of snow crystals as a case study in crystal growth with the hope that developing a comprehensive mechanistic model for this specific system

*Pasadena, CA 91125

Figure 1. Examples of natural snow crystals exhibiting triangular morphologies. The equivalent diameters range from 1 to 3 mm and are defined by $D = (4A/\pi)^{1/2}$, *where* A *is the projected 2D crystal area. The lower right example shows a crystal with an initial truncated triangular morphology (outlined by the central surface markings) that subsequently grew plate-like branches.*

will shed light on the more general problem of structure formation during solidification (7).

Within the menagerie of known snow crystal morphologies, observers have long documented the occurrence of forms exhibiting a peculiar three-fold symmetry (8), as shown in Figure 1. Scoresby reported triangular forms as early as 1820 (9), and Bentley and Humphreys presented several dozen examples with triangular morphologies in their well-known 1931 compilation of snow crystal photographs (10). Al-

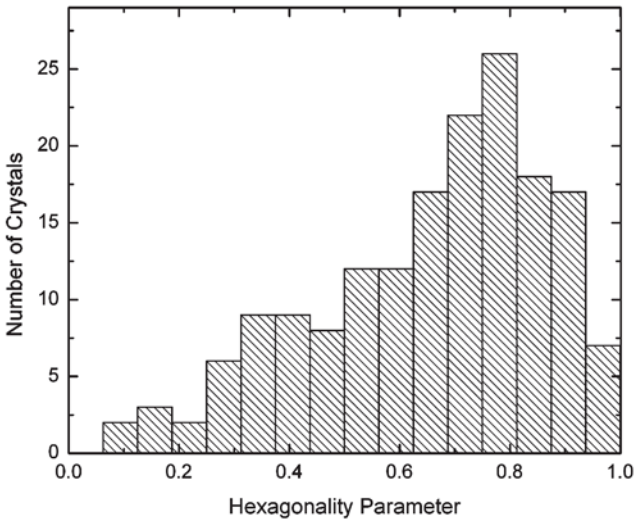

Figure 2. Distribution of laboratory-grown crystals as a function of the hexagonality parameter H. *These data are from an unbiased sample of plate-like crystals grown at -10 °C with a water vapor supersaturation of 1.4%.*

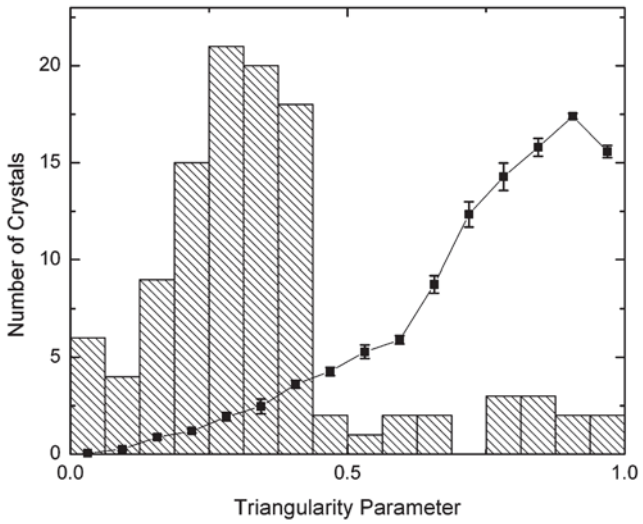

Figure 3. Distribution of laboratory grown crystals with H < *1/3, as a function of the triangularity parameter* T *(bars). The line shows a Monte Carlo model for* T*, described in the text, which assumes random growth perturbations of a hexagonal plate. Error bars show the uncertainty in the model, estimated by varying a number of details in the calculations. The data and model clearly show that crystals with a triangular morphology (small* T*) are much more common than one would expect from random growth perturbations.*

though triangular crystals are usually small and relatively rare, they are visually distinctive and fairly easy to find in nature. While the usual six-fold symmetry seen in snow crystals arises from the intrinsic hexagonal symmetry of the ice crystal lattice, to our knowledge, the formation of triangular shapes has never before been explained.

In this paper, we first present experimental measurements of laboratory-grown ice crystals showing that triangular plate-like crystals do, in fact, form more frequently than would be expected with random growth perturbations. From this data, as well as observations of triangular forms in nature, we conclude that some physical mechanism is required that coordinates the rapid growth of alternating crystal facets. Following this, we then describe an aerodynamic model that explains the growth and stability of triangular snow crystals.

LABORATORY-GROWN CRYSTALS

To examine the phenomenon of triangular snow crystals under controlled conditions, we used a convection growth chamber (11) to produce thin ice crystal plates grown in air at a pressure of one bar. Simple, plate-like snow crystals grown at low supersaturation typically exhibit hexagonal morphologies, but we observed small numbers of crystals with three-fold symmetry at temperatures near -2 °C and between -10 °C and -15 °C (12). Triangular crystals were especially prevalent when grown at a temperature of -10 °C in low water vapor supersaturations, so all the data shown below were taken at -10 °C with a supersaturation of 1.4%. Under these conditions, approximately 5% of the plate-like crystals we observed had a truncated triangular appearance, and examples with nearly perfect equilateral-triangle morphologies were readily found.

We first looked at the prevalence of triangular and other nonhexagonal morphologies by nucleating crystals in our chamber and recording video images of an unbiased sampling of all plate-like crystals that fell on a substrate at the bottom of the chamber after 5-10 minutes of growth in free fall. We ignored nonplate-like, blocky forms, which are present in relatively small numbers at this temperature (12).

We defined a "hexagonality" parameter $H = L_1/L_6$ for the crystal plates, where L_1 and L_6 are the lengths of the shortest and longest prism facets, respectively. H is close to unity when a plate is nearly hexagonal, while H is smaller for any of a variety of odd-shaped plates. Figure 2 shows the measured H distribution for an unbiased sample from our data. Crystals with $H > 3/4$

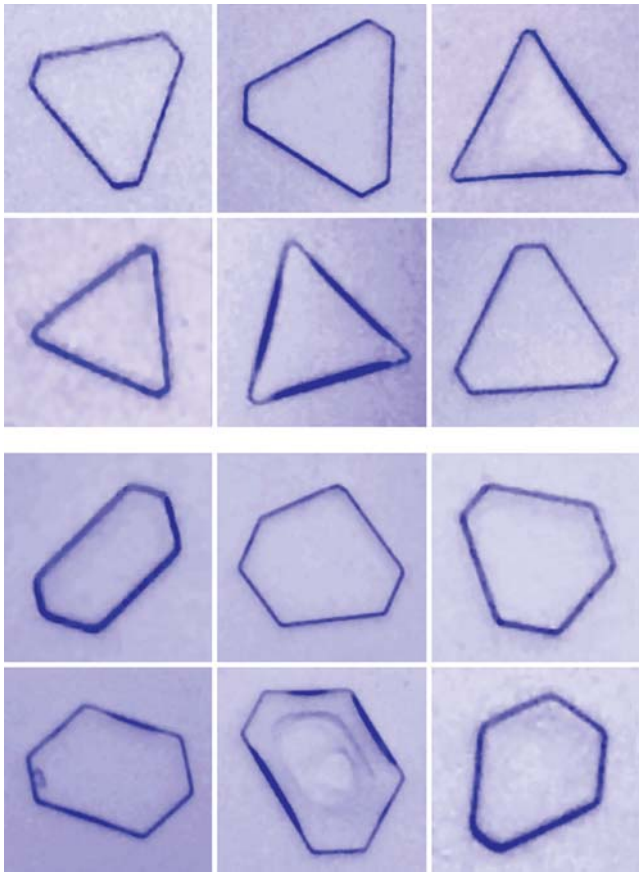

*Figure 4. Examples of some extreme (*H < *1/3) crystal morphologies. The top six images show crystals with* T < *1/2, while the bottom six show crystals with* T > *1/2. The former were more common than the latter, as can be seen from Figure 3. Equivalent diameters ranged from roughly 50 to 100 μm.*

appeared nearly hexagonal to the eye, and this plot shows that the crystals in our sample were mostly hexagonal with relatively small distortions. We say a plate-like crystal has an "extreme" morphology (far from hexagonal) if $H < 1/3$.

From the subset of extreme crystals, we then measured a "triangularity" parameter $T = L_3/L_4$, where L_3 and L_4 are the lengths of the third and fourth smallest facets, respectively. This parameter was small if, and only if, the morphology was that of a truncated triangle, and we observed $T \rightarrow 0$ if, and only if, the morphology was nearly that of an equilateral triangle. Figure 3 shows the T distribution for extreme crystals only. Most of the extreme plate crystals were clearly in the shape of truncated triangles to the eye, and this is reflected in the fact that the T distribution is skewed to lower values. Figure 4 shows a sample of some of the extreme crystals we observed in our data.

We used a simple Monte Carlo simulation to investigate the null hypothesis that our observations were due entirely to random variations in the growth rates of the different prism facets. We generated crystals for which the perpendicular growth velocity of each facet was constant and chosen from the same random distribution. We then "grew" these crystals, selected ones with $H < 1/3$, and from many such crystals we generated a T distribution to compare with our data. The results are shown in Figure 3. Here the error bars in the model were estimated by using a variety of sensible random distribution functions (for example, truncated normal distributions with different means and standard deviations) to generate crystal growth rates. In our simulations, random fluctuations in the growth rates of the six facets produced a variety of odd shapes, including trapezoidal, diamond-shaped and other forms. The simulations did not show a preponderance of triangular crystals over other nonhexagonal shapes, in stark contrast to our data.

These considerations provide convincing evidence that, at least under some growth conditions, triangular morphologies are substantially more abundant than one would expect from random fluctuations in the growth of hexagonal plates. From this we conclude that some nonrandom mechanism is responsible for the growth of snow crystal plates with threefold symmetry. In particular, this mechanism must somehow coordinate the growth of the facets so that they alternate between slow and fast growth around the crystal.

AN AERODYNAMIC MODEL

To examine the effects of aerodynamics on snow crystal morphology, first consider the case of a thin hexagonal plate crystal, as shown in Figure 5. The crystal has six prism facets, and each grows outward at some perpendicular growth velocity (in Figure 5, for example, v_{AB} is the growth velocity of the AB facet). For a symmetrical crystal, all six prism facets are the same length and all six growth velocities are equal.

The growth of a faceted crystal is limited partially by water vapor diffusion through the surrounding air and partially by attachment kinetics at the crystal surface. The two effects together result in facet surfaces that are slightly concave at the molecular level (as shown in Figure 5), although they may appear perfectly flat optically (5). Nucleation of new molecular terraces occurs near the corners (points A and B in Figure 5), where the supersaturation is highest. The molecular steps then propagate inward, traveling more slowly near the facet centers where the supersaturation is

lower. The combined effects of surface attachment kinetics and diffusion-limited growth thus automatically establish the concave shape of each facet surface.

The perpendicular growth velocity v_{AB} of the *AB* facet is primarily determined by the nucleation rates near points *A* and *B*. In the symmetrical case, the rates at *A* and *B* are equal, giving the picture shown in Figure 5. If the nucleation rate were slightly greater at *A*, then the picture would be distorted and the facet surface would be tilted slightly relative to the ice lattice. If the nucleation rate at *A* were substantially greater than at *B*, then terraces generated at *A* would propagate all the way across a vicinal surface from *A* to *B* (5). In general, we see that v_{AB} is determined by the greater of the two nucleation rates at *A* and *B*.

As a growing crystal falls, air resistance causes the basal faces to become oriented perpendicular to the fall velocity (i.e., parallel to the ground), as shown in Figure 5. Atmospheric halo observations have shown that thin plate crystals with sizes of order 10-100 μm can orient to within a few degrees of horizontal under ideal conditions (13).

Air flowing around the falling crystal tends to increase growth via the well-known ventilation effect (14). The airflow produces an effective increase in supersaturation where the edges stick out farthest and the resulting flow is the fastest (Figure 5). In the case of a falling plate, this aerodynamic effect mostly increases the growth of the thin edges of the plate (i.e., the prism facets).

With this overall picture in mind, we now consider the case shown in Figure 6. Here we start with a hexagonal plate and assume a small growth perturbation somewhere on the *AB* facet that breaks the sixfold symmetry and makes v_{AB} greater than the other five facet growth rates. This perturbation could come from a crystal dislocation, a step-generating chemical impurity on the surface, a piece of dust, or perhaps some other mechanism. Regardless of the origin of the initial symmetry-breaking perturbation, the larger growth rate v_{AB} initially results in the distorted crystal shape shown as the second stage in Figure 6.

Once this initial asymmetry appears, the additional material produces an increased aerodynamic drag on one side of the plate. This in turn changes the orientation of the falling crystal in such a way that the points *E* and *F* tip downward, toward the fall direction. Relative to the original horizontal orientation, air flowing around the tilted crystal now increases the supersaturation at points *E* and *F* while decreasing it at *A* and *B*. As a result, the nucleation rates at points *E* and *F* increase.

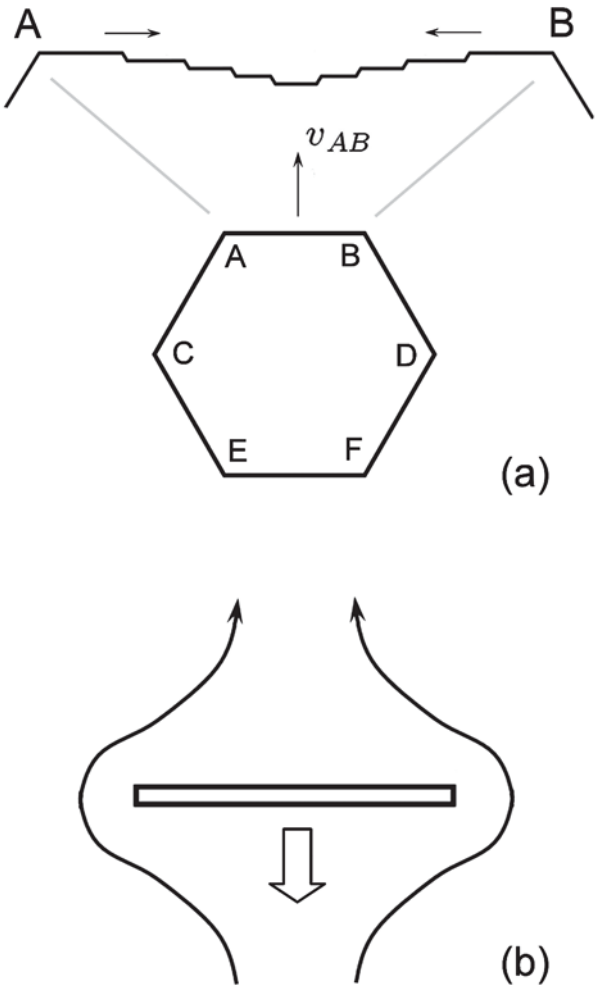

Figure 5. The formation of facets in a simple hexagonal plate-like crystal, as described in the text. The top figure (a) shows a close-up of the AB *facet, exaggerated to show molecular steps on the surface. The bottom figure (b) is a schematic depiction of airflow around a falling hexagonal plate crystal (seen from the side).*

The growth rate of a facet is determined mainly by the greater of the nucleation rates at its two corners (from the discussion of Figure 5 above), and for our tilted crystal we see that the nucleation rates at *E* and *F* must be greater than at *C* and *D*. Thus we must have that $v_{CE} \approx v_{EF} \approx v_{DF}$ to a rough approximation, and furthermore these velocities must all be greater than v_{AC} and v_{BD} (while v_{AB} is somewhat ill-determined throughout because of the assumed growth perturbation). After a period of additional growth in these conditions, shown in the last stage of Figure 6, we find that the length of facet *EF* has increased relative to *CE*

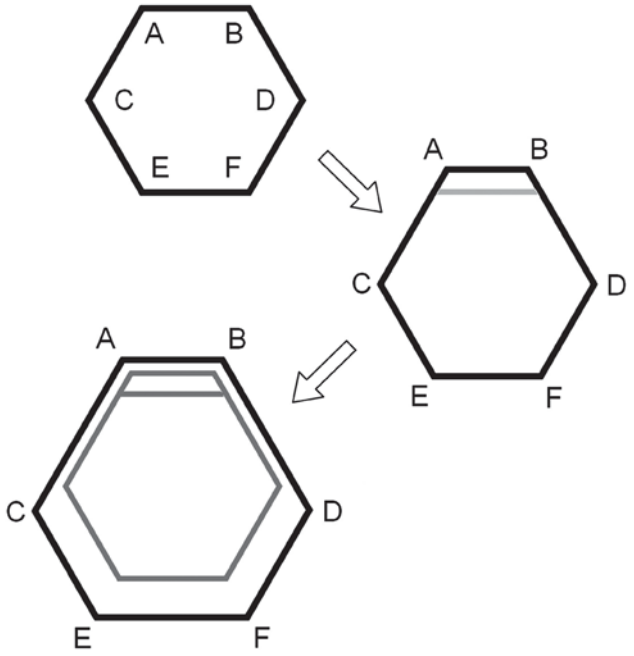

Figure 6. An aerodynamic model for the formation of triangular crystals.

and *DF*. This means that *AB*, *CE* and *DF* are now the three shortest facets, so the crystal has begun to assume a slight triangular shape.

Once aerodynamics produces the shape shown in the last stage of Figure 6, two effects combine to accentuate the triangular morphology. First, the shorter facets (*AB*, *CE*, and *DF* in this case) stick out farther into the supersaturated air, so the Mullins-Sekerka instability (5) tends to increase v_{AB}, v_{CE} and v_{DF} relative to the other three facets. An important aspect of this instability is that it takes less mass to grow a surface of reduced size, so overall mass flow considerations in diffusion-limited growth tend to increase the growth of the shorter facets. Second, airflow is faster around the shorter facets, because they stick out farther, and this also increases their growth relative to the longer facets via the ventilation effect.

The end result is that an initial symmetry-breaking perturbation results in a growth morphology that becomes more triangular with time. Only one initial perturbation is necessary, and no coordination intrinsic to the molecular structure of the crystal need be present. The coordination of the growth rates of alternating facets is brought about by the aerodynamics of the falling crystal.

An interesting feature of our model is that a triangular plate morphology is both aerodynamically stable, and it is stable against additional growth perturbations. Once a plate takes the form of an equilateral triangle ($T \rightarrow 0$), subsequent growth perturbations cannot change the morphology, as long as the plate remains faceted. This is not true for hexagonal plates, so even small initial perturbations would eventually result in triangular shapes. This triangular growth instability is weak, however, so it would not be a dominant effect under typical conditions.

The tendency to form triangular crystals is enhanced if the growth rate increases rapidly with increasing supersaturation, as this accentuates the growth differences resulting from aerodynamic effects. The condensation coefficient increases especially rapidly with supersaturation at -10 °C (15), so it is likely this is why our observations at -10 °C yielded an especially high fraction of triangular crystals.

CONCLUSIONS

Observations of natural snow crystals have long suggested that triangular morphologies are more common than one would expect from random growth perturbations, and that triangular forms are generally more common than other nonhexagonal plates. This conclusion is strongly reinforced by our measurements of laboratory-grown crystals. Since a trigonal symmetry is not present in the underlying crystalline lattice, some external mechanism is required to explain the formation of these crystals.

We believe that the aerodynamic model described above explains the occurrence of snow crystal plates with triangular morphologies, both in the lab and in nature. In particular, this mechanism qualitatively shows how a single symmetry-breaking perturbation in a hexagonal plate can result in the growth of a triangular morphology.

Unfortunately, producing a more complete, quantitative aerodynamic model will be difficult. Researchers have only recently developed viable numerical techniques for modeling diffusion-limited growth of faceted crystals (16), even for relatively simple physical cases. Adding aerodynamic instabilities and their resulting growth changes in full 3D will likely be a considerable challenge. Nevertheless, even our simple qualitative model makes a number of testable predictions.

As we suggested above, for example, triangular morphologies are more likely to appear when the attachment coefficient is a strong function of supersaturation. Additional measurements at other temperatures and supersaturations would help confirm this behavior. More directly, in situ observations of

electrodynamically levitated crystals (17) could be used to examine the transition from hexagonal to triangular forms in real time, imposing different airflows around the crystal to test many aspects of our aerodynamic model in detail.

Finally, we hope that an improved understanding of the mechanisms controlling ice growth may shed light on other systems, whenever growth is affected by diffusion-limited transport, surface attachment kinetics and particle transport via large-scale flows. The growth of triangular snow crystals is another piece in the puzzle that describes the many interconnected mechanisms by which complex structures emerge spontaneously during solidification.

REFERENCES

1. Prinz, M., Harlow, G. and Peters, J. *Simon & Schuster's Guide to Rocks & Minerals.* Simon & Schuster: New York, 1978.

2. Imai, H. *Self-Organized Formation of Hierarchical Structures*. Springer-Verlag: Berlin, 2007.

3. Kolasinski, K.W. "Solid structure formation during the liquid/solid phase transition." *Current Opinions in Solid State & Materials Science*, **11,** pp 76-85, 2007.

4. Ben-Jacob, E. and Garik, P. "Ordered shapes in nonequilibrium growth." *Physica D*, **38,** pp 16-28, 1989.

5. Saito, Y., *Statistical Physics of Crystal Growth.* World Scientific: Singapore, 1996.

6. Libbrecht, K.G. *Ken Libbrecht's Field Guide to Snowflakes*. Voyageur Press: St. Paul, MN, 2006.

7. Libbrecht, K.G. "The physics of snow crystals." *Reports on Progress in Physics,* **68 (4),** pp 855-895, 2005.

8. Libbrecht, K.G. *Snowflakes*. Voyageur Press: St. Paul, MN, 2008.

9. Scoresby, W. *An Account of the Arctic Regions with a History and Description of the Northern Whale-Fishery*. Archibald Constable Publishing: London, 1820.

10. Bentley, W.A. and Humphreys, W.J. *Snow Crystals*. McGraw-Hill: New York, 1931.

11. Libbrecht, K.G. and Morrison, H.C. "A Convection Chamber for Measuring Ice Crystal Growth Dynamics." arXiv.org, Cornell University Library, arXiv:0809.4869, 2008.

12. Libbrecht, K.G., Morrison, H.C. and Faber, B. "Measurements of Snow Crystal Growth Dynamics in a Free-fall Convection Chamber." arXiv.org, Cornell University Library, arXiv:0811.2994, 2008.

13. Tape, W. *Atmospheric Halos*. Antarctic Research Series, Vol. 64. American Geophysical Union, 1994.

14. Keller, V.W. and Hallett, J. "Influence of air velocity on the habit of ice crystal growth from the vapor." *Journal of Crystal Growth,* **60,** pp 91-106, 1982.

15. Libbrecht, K.G. and Arnold, H.M. In preparation.

16. Gravner, J. and Griffeath, D. "Modeling snow-crystal growth: A three-dimensional mesoscopic approach." *Physics Review E,* **79 (1),** id. 011601, 2009.

17. Swanson, B.D., Bacon, M.J., Davis, E.J., et al. "Electrodynamic trapping and manipulation of ice crystals." *Quarterly Journal of the Royal Meteorological Society*, **125,** pp 1039-1058, 1999.